Reconfigurable 2D optical tapped-delay-line to perform correlation on images

Mohammad Reza Chitgarha,[1,*] Morteza Ziyadi,[1] Salman Khaleghi,[1] Amirhossein Mohajerin-Ariaei,[1] Ahmed Almaiman,[1] Joseph D. Touch,[2] Moshe Tur,[3] Carsten Langrock,[4] Martin M. Fejer,[4] and Alan E. Willner[1]

[1]*Department of Electrical Engineering, University of Southern California, Los Angeles, California 90089, USA*

[2]*Information Sciences Institute, University of Southern California, 4676 Admiralty Way, Marina del Rey, California 90292, USA*

[3]*School of Electrical Engineering, Tel Aviv University, Ramat Aviv 69978, Israel*

[4]*Edward L. Ginzton Laboratory, Stanford University, Stanford, California 94305, USA*

**Corresponding author: chitgarh@usc.edu*

Received July 23, 2014; revised October 14, 2014; accepted October 19, 2014;
posted October 22, 2014 (Doc. ID 217645); published November 17, 2014

We demonstrate a reconfigurable 2D optical tapped-delay-line (OTDL) to correlate quadrature-phase-shift-keying (QPSK) 20 Gbaud data. By implementing two independent tapped-delay-lines which performs correlation over rows (inner sum), along with a coherent multiplexing of the correlated rows which performs correlation over columns (outer sum), a 2D correlator is achieved with average error vector magnitude (EVM) of ~7.8%. Here we also search different 2×2 patterns in a 31×31 image and successfully recognize the target patterns in the image. © 2014 Optical Society of America

OCIS codes: (060.2360) Fiber optics links and subsystems; (060.4370) Nonlinear optics, fibers; (190.4223) Nonlinear wave mixing.

http://dx.doi.org/10.1364/OL.39.006573

Signal correlation is a fundamental function in both analog and digital signal processing. Its applications range from matched filtering and decoding, to pattern (header) recognition, packet switching, and image processing [1–3]. The implementation of correlators typically generates signal copies and obtains a weighted sum of these copies to find the desired pattern. There might be a benefit to performing correlation in the optical domain so that the function can be performed at the line rate at which the data is arriving [4]. Moreover, valuable features of an optical correlator (e.g., tunability, reconfigurable target patterns, high bit rate) can be achieved using all-optical signal processing.

Given the recent advances in coherent and phase-modulated systems, correlation in the amplitude and phase domains might yield higher correlation rates, correlation resolution, and efficiency. A correlator can be implemented using the tapped-delay-line (TDL) structure. To search for the target pattern in an incoming data stream, TDL coefficients are set to the conjugate of the target pattern, the data stream slides through the TDL taps, and adjacent symbols are multiplied by the tap coefficient and added to form the output. The output will then need further processing to detect the correlation peaks [5,6].

Tunable optical correlators on a 1D data stream have been demonstrated for both amplitude modulation and phase modulation formats with complete tunability over the data rate and target pattern [7–9]. Furthermore, a recent report showed the ability to perform correlation on multiple WDM channels independently. However, there are applications in which there exists a 2D data space that would require correlation, such that data has encoding or a pattern across 2 independent dimensions. Examples include (a) coding across different domains, such as time and wavelength, and (b) 2D image processing. A laudable goal would be to show that a high-speed, tunable and reconfigurable optical correlator can function to locate a pattern within a 2D space. One approach to perform 2D correlator can be using time to space conversion schemes, and applying Fourier optics for pattern searching [10].

In this report, we demonstrate a reconfigurable 2D optical tapped-delay-line (OTDL) to correlate quadrature-phase-shift-keying (QPSK) 20-Gbaud data. By implementing a WDM TDL on two different signals which performs correlation over rows (inner sum), along with a coherent multiplexing of WDM channels which performs correlation over columns (outer sum), a 2D correlator is achieved with average error vector magnitude (EVM) ~7.8%. Here we also search for different 2×2 patterns in a 31×31 image and successfully recognize the target patterns in the image.

The conceptual block diagram of the 2D OTDL is shown in Fig. 1. First, each image row is mapped to a WDM data channel by modulating optical frequency comb lines (phase-locked sources) with QPSK symbols corresponding to the color of the image pixels. Second, a WDM-TDL performs a 1D correlator on each data channel independently and generates the inner sums on each of them with the given coefficients (b_i). Subsequently, these processed WDM channels—which are phase coherent—are multiplexed together with column coefficients (a_i) to generate the outer sums. The output is then processed to find the correlation peaks and the positions of the matched pattern.

In our proposed 2D OTDL, a highly nonlinear fiber (HNLF), and two periodically-poled-lithium-niobate (PPLN) waveguides are used for performing the WDM TDL and for realizing coherent multiplexing. A conversion-dispersion-based delay is realized in a spool of dispersion-compensating fiber (DCF) to induce a relative delay between the data channels [11].

First, in order to transfer the image pixels of four colors into the WDM data channels first multiple frequency comb lines that are located equidistantly are modulated

 © 2014 Optical Society of America

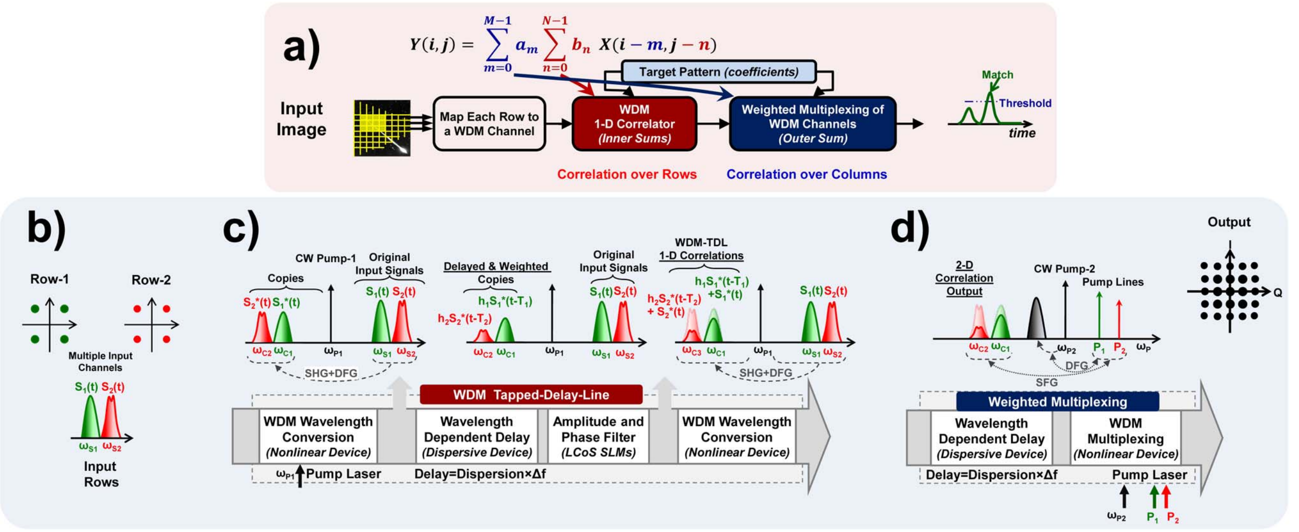

Fig. 1. (a) Block diagram a 2D TDL with two cascaded 1D correlators to perform 2D correlation the images. Operational principle of the 2D correlator: (b) First the image pixels are serialized and modulated in different frequencies. (c) Then, independent correlations are performed on all rows. (d) Finally all processed rows are combined coherently to complete a 2D correlation.

with a single QPSK modulator with symbol duration T_s. This modulator is driven by the data with four possible symbols corresponding to the four colors of the image ($X(t)$). To encode the $N \times N$ 2D image data onto the comb lines, the data needs to be serialized in such a way that the first row comes first. Then, a conversion-dispersion delay is used to induce a relative delay of NT_s so that each data channel corresponds to one row.

The 2D OTDL consists of two cascaded inner and outer products. To realize the inner product of the 2D correlator, the WDM channels (which represent the image rows) are sent into an HNLF together with a high-power continuous-wave (CW) pump, producing one phase-conjugated copy of each signal through four-wave mixing (FWM) process that lands on a new frequency that is different from the original signal (i.e., $\omega_{\mathrm{Ci}} = 2\omega_{P1} - \omega_{\mathrm{Si}}$). Then, the WDM signals and the WDM copies are sent to a dispersive element (e.g., dispersion compensating fiber, DCF), and a relative delay of $T_i = D \times (\lambda_{\mathrm{Si}} - \lambda_{\mathrm{Ci}})$ is introduced between the signal and its copy (i.e., conversion-dispersion optical delay). All the signals, delayed copies, and the CW pump are then sent to an in-line phase and amplitude-programmable filter to change the amplitude and relative phase of the signal copies. This is equivalent to a complex-coefficient of $|b_i|e^{j\measuredangle b_i}$ on the signal copies. All the signals and the pump are kept on the same fiber path, preserving phase coherence between the channels. When these signals travel through the second nonlinear stage (e.g., PPLN waveguide), the original signals again copy themselves to the ω_{Ci} frequencies. This new copy, which lands on the old copy, is phase coherent with the old copy and has a different delay and different weight. This creates a 2-tap TDL for each WDM data signal with independent control over the tap coefficients. In the PPLN waveguide, the CW pump laser, located at quasi-phase-matching (QPM) wavelength ω_0, is mixed with itself through second-harmonic-generation (SHG), and then creates the second copy of each WDM data channel through difference-frequency-generation (DFG) at ω_{ck} ($\sum_{i=1}^{2} b_i s_k (t - iT_s)$ where $s_k(t) = X(t - kNT_s)$).

To realize the outer sum, all correlated rows need to be multiplexed together coherently. Therefore, the processed rows, another set of coherent comb lines with the same frequency spacing and a CW pump laser ω_{P2}, are injected into the third nonlinear device (a PPLN waveguide) to perform the coherent addition, which corresponds to the outer sum. Here, the complex coefficients are $|a_k|e^{j\measuredangle a_k}$ which can be applied on the pump lines.

$$y(t) = \sum_{k=1}^{2} a_k \sum_{i=1}^{2} b_i X(t - (kN + i)T_s). \qquad (1)$$

Figure 2 shows how vector addition of the QPSK symbol in the proposed correlator can be used to find the target pattern. In each row, the incoming consecutive two QPSK symbols are multiplied with the conjugate of

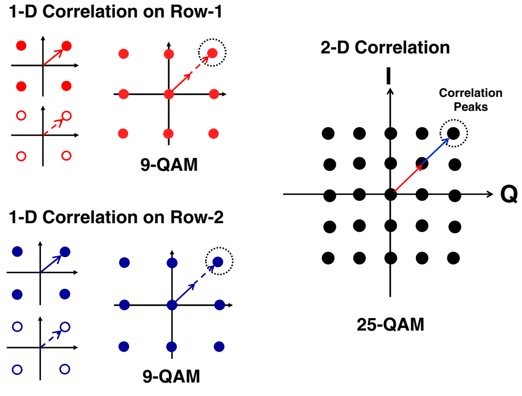

Fig. 2. Vector addition of two QPSK data channels in first and second rows and generation of 9-QAM signal. A 25-QAM signal is created by combining two processed rows. The matched pattern corresponds to the symbol in the upper-right corner of the IQ constellation plane of the correlator output.

the target pattern and added together to create a 9-quadrature-amplitude modulation (9-QAM). Only one of these 9 possible symbols (i.e., the upper right corner) corresponds to the target pattern in that row. Subsequently, the generated 9-QAM signals are combined to create a 25-QAM after applying the coefficient associated to the outer sum weights. The symbol in the upper right corner of the constellation plane is matched to the 2D target pattern. In general, if the target pattern is an $N \times M$ 2D block, for each row, the correlated output is in the form of an $(M+1)^2$-QAM, which will be converted to an $(M+N+1)^2$-QAM after combining with the other $N-1$ rows. Therefore, the size of the target pattern (i.e., $M+N$) is limited to the coherent receiver's ability to detect the $(M+N+1)^2$-QAM.

The experimental setup for the 2D OTDL is depicted in Fig. 3. A mode-locked laser with a 10-GHz repetition rate is used to generate coherent comb lines with 10-GHz frequency spacing. A delay-line-interferometer (DLI) with FSR 20 GHz is used to double the frequency spacing of the comb lines. The 20-GHz comb is then passed through an HNLF fiber to generate a flat and broad spectrum. The output of the HNLF is sent to a liquid crystal on silicon (LCoS-1) filter to select and write complex weights on the comb lines and separate them into a signal path (orange path) and a pump path (green path). Two pairs of comb lines with ~1.6 nm separation are selected for the signal path (i.e., 1543.3 and 1544.9 nm) and for the pump path (i.e., 1543.6 and 1545.2 nm). Next, the comb lines on the signal path are sent to a nested Mach–Zehnder modulator to generate the 20 Gbaud QPSK data (PRBS $2^{31}-1$ or predetermined pattern). To form the two modulated signals as two consecutive rows in a 31×31 image, they must be sent to DCF-1 of 12 km in length to induce ~969 ps/nm dispersion (31 symbols of delay). The resulting signals are amplified together in an EDFA, combined with an amplified ~1550 CW pump, and sent to a 450-m HNLF with zero dispersion wavelength of around 1555 nm to produce the first copies at 1555.2 and 1556.8 nm. All signals then travel through a ~70 m DCF and LCoS-2 to apply tap delays, phases, and amplitudes. The DCF-2 introduces around one symbol time of relative delay between the signals and the copies. The output of the DCF-2 is then sent to a 4-cm-long PPLN waveguide to create the second copies at the same wavelengths and complete the inner sum. The quasi-phase-matching (QPM) wavelength of the first PPLN waveguide is temperature-tuned to the CW pump wavelength (i.e., 1550 nm). The generated copies at 1555.2 and 1556.8 nm are filtered and combined with the comb lines selected for the pump path and another CW laser at ~1548.6 nm pump, and sent to the second PPLN (5 cm in length) with QPM wavelength 1550.15 nm after sufficient amplification to perform coherent multiplexing of the copies at ~1551.7 nm. The pump lines also pass back through the DCF-1 to stabilize the generated signal. The multiplexed signal is then filtered and sent to the coherent receiver, after passing through another DCF of the same length to compensate for the induced dispersion. In this demonstration, the polarization state can be stabilized by using polarization maintaining (PM) fiber.

Figure 4 depicts the output spectra of the WDM OTDL stages for a 20 Gbaud QPSK 2D correlator. In the first stage, a CW laser creates a conjugate copy for each WDM data signal that corresponds to a 1-tap TDL in each row. In the second stage, on both rows, a 2-tap correlation is performed independently by applying appropriate amplitudes, phases, and delays in the programmable filter and the subsequent DCF on the conjugate copies. As shown, the two 9-QAM signals (9 possible correlation results) are thus generated by combining two QPSK (4-QAM) signals.

In the last nonlinear stage, these two signals are multiplexed coherently with the column coefficients to realize a 2D correlator. In Fig. 5(a), the spectrum of the second PPLN waveguide is depicted. In this stage, two processed rows are combined with appropriate amplitudes and phases correspond to the 2D target pattern and generate a 25-QAM constellation (25 possible correlation results). These results are shown in Figs. 5(b)–5(d). Figure 5(b) shows the 25-QAM correlation results for the target

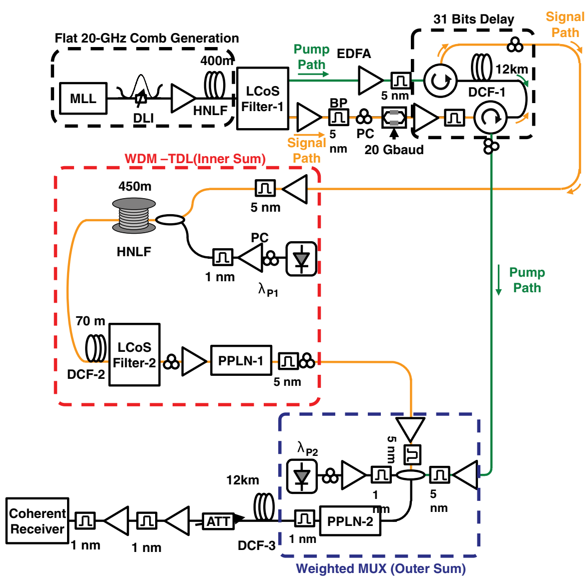

MLL: Mode-locked laser
MZM: Mach-Zender modulator
DCF: Dispersion compensating fiber
PC: Polarization controller
DLI: Delay line interferometer
BPF: Bandpass filter

Fig. 3. Experimental setup for the proposed optical 2D correlator. A mode-locked laser is used to generate coherent frequency comb lines.

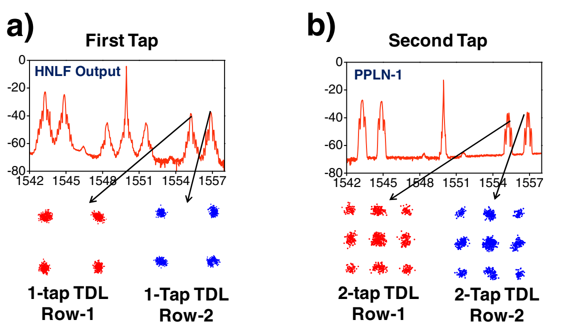

Fig. 4. WDM OTDL performed two independent 2-tap correlators on both rows; (a) spectrum of the HNLF output showing the first tap of 1-tap TDL on row-1 and row-2, with 4-QAM constellation; and (b) spectrum of the PPLN-1 output, showing the 2-tap TDL on row-1 and row-2 with 9-QAM constellation.

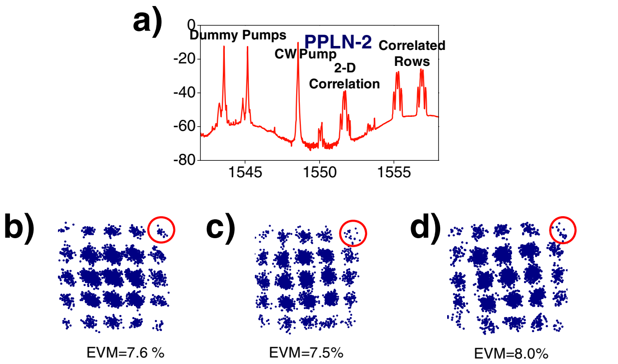

Fig. 5. (a) Spectrum of the PPLN-2 output in which coherent multiplexing of the processed rows has taken place and the 25-QAM constellations of the proposed correlator for different target patterns with EVMs of (b) 7.6%, (c) 7.5%, and (d) 8% are obtained. The point in the upper right corner of the IQ plane corresponds to the matched pattern.

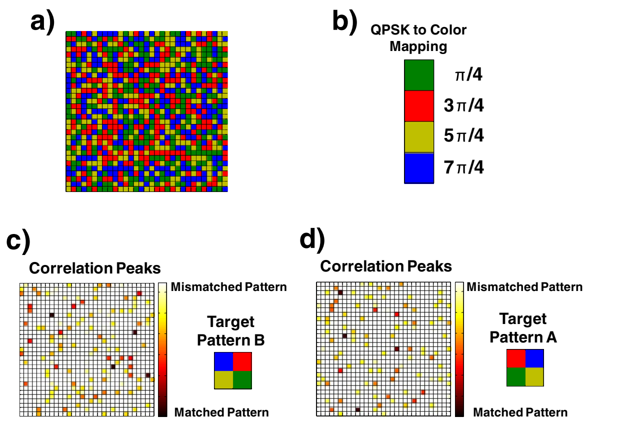

Fig. 6. (a) Original four-color 31×31 image, (b) color to symbol mapping. Searching for two different 2×2 target patterns in an image with 961 pixels in 6(c) and 6(d). The correlation peaks are obtained with respect to the upper-right corner of the 25-QAM constellation. The dark squares correspond to the target.

pattern of $\begin{bmatrix} \pi/4 & \pi/4 \\ -(3\pi/4) & 3\pi/4 \end{bmatrix}$ with an EVM of 7.6%. The point in the upper right corner of the IQ plane corresponds to the matched pattern. Figures 5(c) and 5(d) shows the similar results with EVMs of 7.5% and 8% and the search patterns of $\begin{bmatrix} \pi/4 & 3\pi/4 \\ -(3\pi/4) & \pi/4 \end{bmatrix}$ and $\begin{bmatrix} -(\pi/4) & -(\pi/4) \\ -(3\pi/4) & 3\pi/4 \end{bmatrix}$, respectively.

In Fig. 6, an image is searched for two different patterns. Fig. 6(a) shows a 31×31 image (961 pixels) where each pixel can be one of four possible colors. The image pixels can be transferred to a QPSK data channel by mapping each color to a QPSK symbol according to Fig. 5(b). In order to serialize the 2D image data, the relative delay between two WDM channels is set to $31 \times 50 = 1550$ ps. The total length of the data is 961 symbols, which can be programmed in the pattern generator. Fig. 6(c) and 6(d) shows the 2D correlator output after offline processing. The matched patterns are located in the upper-right corner of the IQ plane, so the inverse of the distance between correlation results and the upper-right point in the IQ plane determines the amount of similarity between each 2×2 section of the image and the 2×2 target pattern. These distances are mapped to the colors in a 31×31 table for both Fig. 6(c) and 6(d). Therefore, the darkness of each pixel here indicates the amount of similarity between the 2×2 section of the original image starting at that pixel with the 2D target pattern. These results are depicted for two target patterns $\begin{bmatrix} -(\pi/4) & 3\pi/4 \\ -(3\pi/4) & \pi/4 \end{bmatrix}$ and $\begin{bmatrix} 3\pi/4 & -(\pi/4) \\ \pi/4 & -(3\pi/4) \end{bmatrix}$ in Figs. 6(c) and 6(d), respectively. As shown, the experimental results for both patterns exhibit 4 peaks (dark points) in each table at the 2×2 sections that are matched to the target patterns.

This work was made possible by support from NSF, CIAN, DARPA, and Cisco Systems.

References

1. A. V. Oppenheim, R. W. Schafer, and J. R. Buck, *Discrete- Time Signal Processing* (Prentice Hall, 1999).
2. J. G. Proakis, *Digital Communications* (McGraw-Hill, 2000).
3. J. S. Lai, *Two-Dimensional Signal and Image Processing* (Prentice Hall, 1990).
4. B. Moslehi, J. W. Goodman, M. Tur, and H. J. Shaw, Proc. IEEE **72** 909 (1984).
5. M. S. Rasras, I. Kang, M. Dinu, J. Jaques, N. Dutta, A. Piccirilli, M. A. Cappuzzo, E. Y. Chen, L. T. Gomez, A. Wong-Foy, S. Cabot, G. S. Johnson, L. Buhl, and S. S. Patel, IEEE Photon. Technol. Lett. **20**, 694 (2008).
6. C. R. Doerr, S. Chandrasekhar, P. J. Winzer, A. R. Chraplyvy, A. H. Gnauck, L. W. Stulz, R. Pafchek, and E. Burrows, J. Lightwave Technol. **22**, 249 (2004).
7. Y. Dai, Y. Okawachi, A. C. Turner-Foster, M. Lipson, A. L. Gaeta, and C. Xu, Opt. Express **18**, 333 (2010).
8. S. Khaleghi, O. F. Yilmaz, M. R. Chitgarha, M. Tur, N. Ahmed, S. Nuccio, I. Fazel, X. Wu, M. W. Haney, C. Langrock, M. M. Fejer, and A. E. Willner, IEEE Photon. J. **4**, 1220 (2012).
9. M. R. Chitgarha, S. Khaleghi, O. F. Yilmaz, M. Tur, M. W. Haney, C. Langrock, M. M. Fejer, and A. E. Willner, Opt. Lett. **38**, 2271 (2013).
10. D. F. Geraghty, R. Salem, M. A. Foster, and A. L. Gaeta, IEEE Photon. Technol. Lett. **20**, 487 (2008).
11. M. R. Chitgarha, M. Ziyadi, S. Khaleghi, A. Mohajerin-Ariaei, A. Almaiman, J. Touch, M. Tur, C. Langrock, M. M. Fejer, and A. E. Willner, *European Conference on Optical Communications (ECOC)* (2013), paper Tu.1.C.6.